The Seismic Network of Chile

by S. Barrientos and National Seismological Center (CSN) Team

ABSTRACT

Chile is frequently affected by large and potentially tsunamigenic and damaging earthquakes as a result of rapid convergence of the Nazca plate beneath the South America plate. Ten **M** 8 or larger earthquakes have occurred along the Chilean coast in the past century, the largest of which was the 1960 **M** 9.5 Valdivia earthquake. After the 2010 **M** 8.8 Maule earthquake, Chile began installing a modern real-time network of digital broadband/strong-motion and Global Positioning System (GPS) stations to better prepare for future and expected large damaging earthquakes. The network was designed to provide fast and accurate estimates of earthquake source parameters of potentially devastating earthquakes for emergency response applications, and was also capable of comprehensive characterization of Chilean seismicity necessary for long-term hazard assessment and mitigation activities. Beginning in 2013, the National Seismological Center (CSN) of the University of Chile was mandated by the Chilean government to implement a network of 65 permanent real-time broadband and strong-motion stations and 130 Global Navigation Satellite Systems (GNSS) monuments and receivers. These integrated sensor systems were designed to provide accurate automatic earthquake locations and magnitudes necessary for tsunami warning and impact assessment. In near-real-time applications, the GPS stations become critical for determination of fault finiteness of **M** ~ 7 or larger earthquakes. Operations of these systems also provide new insights into long-term deformation and associated spatiotemporal variations in seismicity, which are necessary in long-term earthquake hazards assessment and mitigation. In addition to the real-time system described above, 297 strong-motion offline instruments complement the network for engineering purposes. Broadband data in real time are publicly available through the Incorporated Research Institutions for Seismology Data Management Center (IRIS-DMC) under networks C and C1. Strong-motion data for recorded accelerations larger than 2%*g* are available through the CSN webpage.

INTRODUCTION

Chile is among the most seismically active countries in the world. Since the arrival of the Spaniards, who started the written record in mid-1500s, a magnitude (**M**) 8 or more earthquake has taken place approximately every dozen years. In the last 100 yrs, 10 events **M** ~ 8 or larger have taken place in this region. Three events with **M** > 8 have occurred within the past 7 yrs. Historical records of local damage, reports of tsunami heights recorded in Japan, and recent paleoseismological studies have evidenced several earthquakes with **M** near or exceeding 9. Among them is the 1960 event, the largest earthquake recorded since the beginning of instrumental seismology. Such extreme seismic activity is the result of the interaction of the Nazca, Antarctic, Scotia, and South American plates in southwestern South America, where Chile is located (Fig. 1).

Several seismogenic zones are recognized in Chile based on the analyses of large earthquakes, the hypocentral locations of earthquakes large enough to be recorded at teleseismic distances, and studies of smaller earthquakes carried out with recent permanent and temporary local networks (Fig. 2):

1. Nazca–South America coupling region. Large thrust earthquakes at shallow depths, because of their relatively high frequency of occurrence, are responsible for most of the damage recorded in history. They are located along the coast from Arica (18° S, the northernmost extreme of coastal Chile) to the triple junction at Taitao Peninsula (46° S). These events take place as a result of the convergence of the Nazca beneath the South American plate at a rate of about 6.5 cm/yr. Farther south, the Antarctic plate subducts beneath the South American plate at a rate of ~1.8 cm/yr.

   M 8 or larger earthquakes are usually accompanied by notable coastal elevation changes and, depending on the amount of seafloor vertical displacement, by catastrophic tsunamis. Their rupture zones extend down to 45–53 km depth (Tichelaar and Ruff, 1991) and their lengths can reach well over 1000 km. The hazard due to these large events is well recognized and understood. Return periods for **M** ~ 8 (and above) events are of the order of 80–130 yrs for any given region in Chile, and about a dozen years when the country is considered as a whole. Megathrust earthquakes seem to have much longer return periods, of the order of a few centuries for any given region (Cifuentes, 1989; Barrientos and Ward, 1990). Recent paleoseismological studies carried out in southern Chile indicate recurrence rates of ~300 yr for these very large earthquakes (Cisternas *et al.*, 2005; Moernaut *et al.*, 2014). Last examples of this type of earthquakes have been the 2010 **M** 8.8 Maule, the 2014 **M** 8.2 Iquique, and the 2015 **M** 8.4 Illapel earthquakes.
2. Intermediate-depth earthquakes. Large intermediate-depth (60–200 km) tensional as well as compressional events within the subducting Nazca plate are a common occurrence. A suite of large magnitude events (**M** around

doi: 10.1785/0220160195

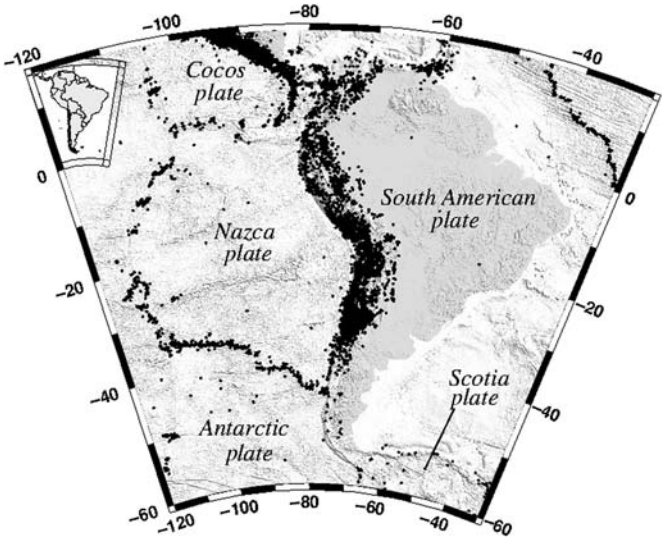

▲ **Figure 1.** Seismicity defining the boundaries of major plates in South America. Less defined, because of less seismic productivity, are the contacts between the South American plate with its two southern boundaries: the Antarctic plate (subduction) and Scotia plate (left-lateral strike-slip fault).

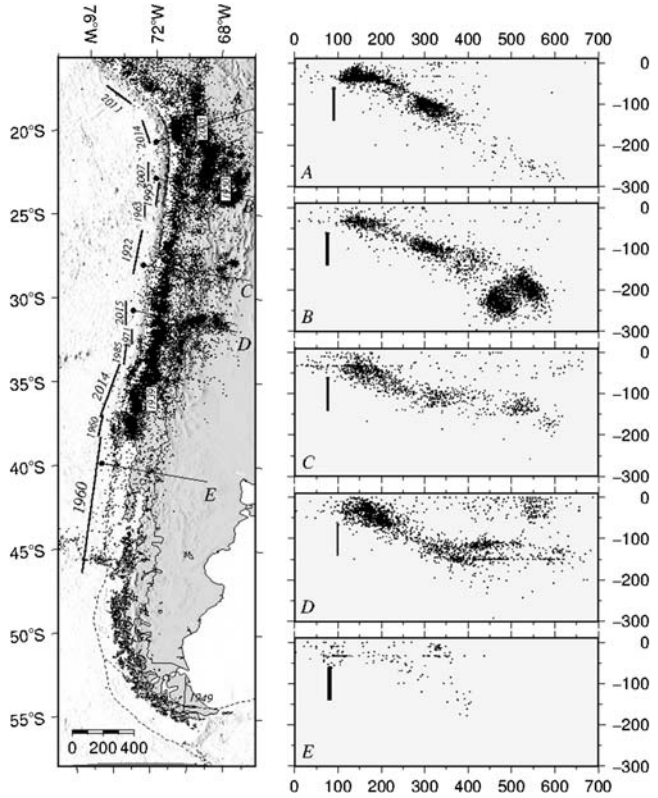

▲ **Figure 2.** (Left) Seismicity of Chile and surrounding regions according to SISRA (1900–1981), U.S. Geological Survey (1982–1999), and National Seismological Center (CSN) (2000–2016) catalog. Estimated rupture length and time of occurrence of large earthquakes along the plate contact are shown to the left of seismicity; number in white boxes show the location of three intermediate depth earthquakes (**M** ~ 8). (Right) Five profiles (A–E) show the depth distribution of earthquakes as a function of distance from the trench.

8) has been reported to occur at depth between 80 and 100 km, all of them associated with extensional faulting: January 1939 **M** 7.8 (Beck *et al.*, 1998), the deadliest earthquake in Chilean history, which produced between 5000 to 28,000 fatalities, and the December 1950 **M** 8.0 (Kausel and Campos, 1992) and the 13 June 2005 **M** 7.7 (Peyrat *et al.*, 2006) earthquakes.

Additionally, complex stress interaction gives rise to down-dip compressional events at about 60–70 km depth, closer to the coast. These events can reach magnitudes over 7, as reported by Lemoine *et al.* (2001) and Pardo *et al.* (2002), in particular for the very damaging earthquake of October 1997 Punitaqui event.

3. Shallow seismicity. Very shallow seismicity (0–20 km) in a few places within the overriding plate, such as the cordilleran region of south–central Chile (Liquiñe-Ofqui fault system) is a consequence of the oblique convergence of the Nazca plate. Magnitudes up to 7.1 have been reported for earthquakes in this region (21 November 1927). The southern extreme of the continent is tectonically dominated by the Magellanes–Fagnano fault system, a left-lateral strike-slip fault resulting from the relative horizontal displacement of the Scotia and South American plates at a rate of the order of 7 mm/yr (Thomas *et al.*, 2003). Two earthquakes of **M** ~ 7.7 each, separated by 8 hrs, were reported in this region on 17 December 1949 and were most likely associated with the Magallanes–Fagnano fault system (Klepeis, 1994; Smalley *et al.*, 2003, 2007).

   Another seismogenic region that has become the subject of recent studies is located at shallow depths in the Andean cordillera in the central part of Chile. Godoy *et al.* (1999) and Barrientos *et al.* (2004) carried out structural and seismicity studies to understand this shallow active region, in which the largest known earthquake (less than 10 km depth) took place on 4 September 1958 (**M** 6.9, Lomnitz, 1960; Alvarado *et al.*, 2009).

   Also, shallow seismicity (h < 20 km) of relative large magnitude (> 5.5) has been recently observed beneath the Andes main Cordillera at latitudes 19.6° S (Aroma; July 2001), 35.8° S (Melado River; August 2004), 38° S (Barco Lagoon; December 2006), and 45° S (Aysén Fjord; April 2007). All these events show significant strike-slip component of displacement.

4. Deeper seismicity occurs further to the east, and can reach up to 650 km depth beneath Bolivia and northwestern Argentina. These events usually present an extensional component along the plate down-dip. The largest known earthquake in this region is the 1994 M_w 8.2 earthquake at 647 km beneath northern Bolivia, which was reported to be felt in Canada and the United States (Frohlich, 2006).
5. Apart from the seismicity associated with the subducting East Pacific Rise approximately at latitude 46° S, outer-rise earthquakes are also present along the subduction margin.

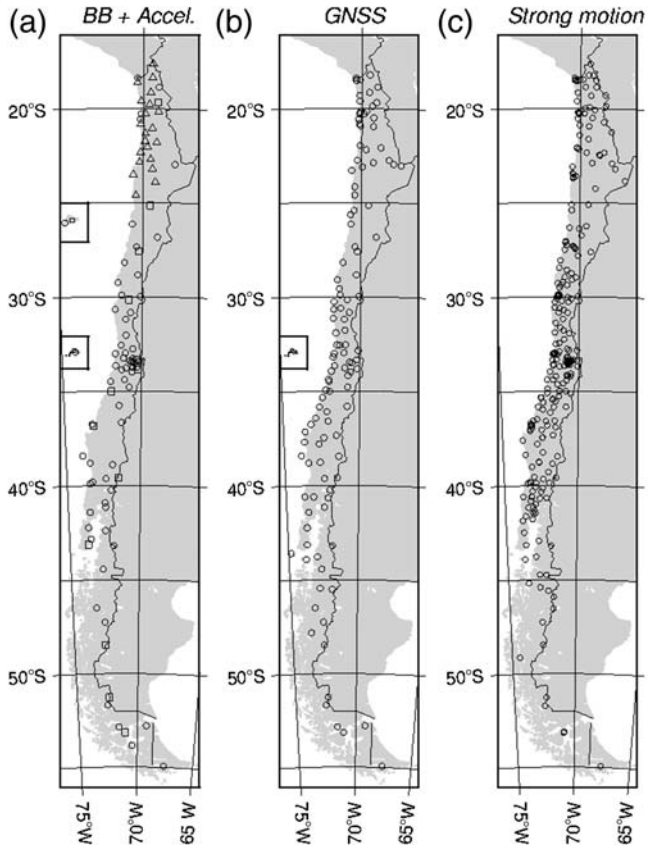

▲ **Figure 3.** Distributions of (a) 105 multiparametric (broadband + accelerographic) stations, (b) 128 Global Navigation Satellite Systems (GNSS) devices, and (c) 297 strong ground motion instruments. An important role in this network is played by 20 Integrated Plate Boundary Observatory Chile (IPOC, open triangles) composed of the CX network in northern Chile, 10 Geophysical Research Observatories stations (GRO, open squares), 3 GSN stations (LCO, LVC, and RPN), and 2 GEOSCOPE stations (PEL and COY).

This seismicity—mainly extensional faulting—is observed seaward beyond the trench. It is particularly evident in south–central Chile, offshore of the 1960 **M** 9.5 giant earthquake (37.5°–46° S) and more recently, offshore of the large coseismic fault displacement associated with the 2010 **M** 8.8 earthquake (34°–37.5° S). The largest aftershock M_w 7.4 of the 2010 sequence belongs to this type of earthquake. Farther north, an M_w 7.0 earthquake of the same type (extension) took place in April 2001, as did aftershocks of the 2015 M_w 8.4 Illapel earthquake.

THE OBSERVATION SYSTEM

The first countrywide observational system was deployed by F. Montessus de Ballore as a consequence of the 1906 Central Chile earthquake, an **M** 8+ event that produced significant damage in Valparaiso and Santiago. The description of the network, with a map indicating the location of the stations, is included in the first issue of the *Bulletin of the Seismological Society of America* (Brenner, 1911). The system included one first-order station (Bosch-Omori, Wiechert, and Stiattesi) located in Santiago, four second-order stations spaced about 800 km along the country, each provided with a horizontal Wiechert pendulum of 200 kg. The system was complemented by 29 third-order Agamennone seismoscopes.

The National Seismological Center (CSN) of the University of Chile, a continuation of the Seismological Service of the Department of Geophysics of the same university, started operations in March 2013. The primary mission of this recently created agency is to install, maintain, and operate a seismic network of 65 multiparametric stations (broadband seismometers, accelerometers, and Global Navigation Satellite Systems [GNSS] devices), 63 GNSS devices recently acquired that augment the existing university network, and those devices contributed through international collaborations. The network is configured to transmit all these data in real time to the central headquarters in Santiago. Complementary to these devices, 297 accelerographs that record strong motion associated with medium to large earthquakes (threshold at 2%g) have been deployed by the Chilean National Office of Emergency, in cooperation with the Ministry of Housing and Urban Planning. These devices were transferred to the CSN in 2015–2016 for their operation and maintenance. The locations of these stations are shown in Figure 3.

All new CSN stations have International Federation of Digital Seismograph Networks network code C1; the older (pre-2013) have code C. The C1 network has 65 stations including broadband velocity (sampled at 100, 40, and 1 samples/s) and acceleration (sampled at 100 samples/s) sensors with six-channel acquisition systems together with GNSS devices sampled at 1 samples/s. In 2017, seven more stations with similar equipment were added to the network, including one 100-m borehole sensor, to monitor possible shallow activity associated with the San Ramon fault, a geologic feature that runs on the eastern border of the capital city, Santiago. Additional stations of the C network (LMEL and ROC1) are sampled at standard configuration 100, 40, and 1 samples/s for broadband channels and 100 samples/s for the acceleration streams.

By design, the new Chilean Seismic Network easily integrates real-time contributions from international research and monitoring partners that include GeoForschungsZentrum (Germany) and Institute de Physique du Globe (France), which form the Integrated Plate Boundary Observatory (IPOC), and Incorporated Research Institutions for Seismology (IRIS) (United States). Each of these partners are contributing seismic observing systems that further expand seismic monitoring and notification capabilities and significantly help in understanding the earthquake potential and addressing earthquake hazards issues.

These IPOC stations are generally composed of displacement (Leica), velocity (STS-2), and acceleration (EpiSensor) sensors with Quanterra acquisition systems. Three streams with sampling rates at all these stations are 100, 20, and 1 samples/s for the BB channels, 100 samples/s for the strong-motion streams, and 1 samples/s at the GNSS sites, apart from the environmental variables.

Ten Geophysical Research Observatories (GRO) stations installed in 2011–2012 part of the C network are roughly equally distributed along the country. These stations are equipped with velocity (STS-2), acceleration (EpiSensor), infrasound (Chaparral) together with environmental sensors (temperature, rain gauge, and pressure) with Quanterra 330 acquisition systems streaming channels at 100, 40, and 1 samples/s.

The locations of each station of these three major elements (a) 105 BB+SGM, (b) 128 GNSS (two stations were vandalized), and (c) 297 SGM stations are shown in Figure 3. The intersensor separation for elements in (a) is about 80–90 km, and elements in (c) are highly concentrated in different sedimentary basins containing cities.

The 128 Trimble GNSS receivers are also part of the network. The system is currently being deployed in the field. Nearly 100 of them are already storing 1 Hz files with connectivity in progress. Forty of these devices include additional RTX capabilities. RTX is the Precise Point Positioning vendor algorithm executed on the receiver by integration of the OmniSTAR-transmitted orbits and clocks corrections.

Initial testing of the RTX system in April 2014 allowed the capture of the first ever record of the Earth's surface displacement produced by an earthquake (aftershock **M** 7.6 of the 1 April sequence) using this technique, about 30 cm of permanent displacement to the west and about 8 cm to the south within 33 s of arrival of the *P* wave (Fig. 4). The first Trimble RTX device was installed at the Iquique airport. Data are transmitted through Dirección General de Aeronáutica Civil (DGAC; Chilean Aeronautic Administration) communications system to Santiago, where it is processed, analyzed, and archived.

Because the seismological observation system developed by the CSN is the only system at a national scale, it must fulfill several objectives.

1. *Rapid characterization of large earthquakes*: The network must be capable of providing enough information to rapidly characterize large earthquakes in Chile, particularly to evaluate the potential generation of tsunamis in the near field. This is not a simple task because large magnitude earthquakes (**M** > 8) take place very close to the observation system. Systems based on broadband seismometry are saturated in the near field whereas recorded acceleration doubly integrated to displacement is often unstable because it requires accurate baseline corrections and proper estimations of rotations and tilts (Kinoshita and Takagishi, 2011; Wang *et al.*, 2011; Colombelli *et al.*, 2013). Because the near-field terms of the displacement at the surface of a half-space decay very rapidly as a function of distance from the source, it is extremely desirable that GNSS stations are located as close as possible to the rupture. To capture the large earthquakes along the coupling region of the Nazca and South American plates between the coast and the trench, a surface that can be represented by the SLAB1.0 model (Hayes *et al.*, 2012), the GNSS stations are deployed roughly every 40–50 km along the coast. This allows an intersensor spacing of the same order of the depth to the seismogenic region, ~40 km. Inland, a sparser distribution of stations is sufficient, complementing instrumentation at the recently installed BB stations.
2. *Seismogenic zones definition*: A second objective is to define—to the best possible extent—the seismogenic zones that are responsible for the earthquake hazard in Chile. The network must have enough sensitivity to detect earthquakes of magnitude 3.5 and above within the country. It is recognized that even smaller earthquakes could provide a better definition of these sources in shorter time intervals, but the existing network of roughly 80–90 km sensor interspacing can indicate regions where to concentrate future efforts with denser arrays.
   To estimate the completeness magnitude of the network, Gutenberg–Richter relations have been calculated for the years 2013–2016 (Fig. 5). Aftershocks of the 2014 Iquique and the 2015 Illapel earthquakes have not been removed. For these three years, the curves reveal that the completeness magnitude (the magnitude at which the frequency–magnitude distribution departs from the linear Gutenberg–Richter relation) is of the order of 3.5 and *b*-values range from 0.78 (2014) to 0.95 (2015). According to the data, there were ~10 events with magnitude larger than 6.5 during the last three years in Chile.
3. *Strong motion characterization*: The Ministry of Housing and Urban Planning and the Office of Emergency of the Interior Ministry deployed 297 strong motion instruments, which have been transferred to the CSN to provide a reliable database of strong-motion records (accelerations) produced by large earthquakes for engineering

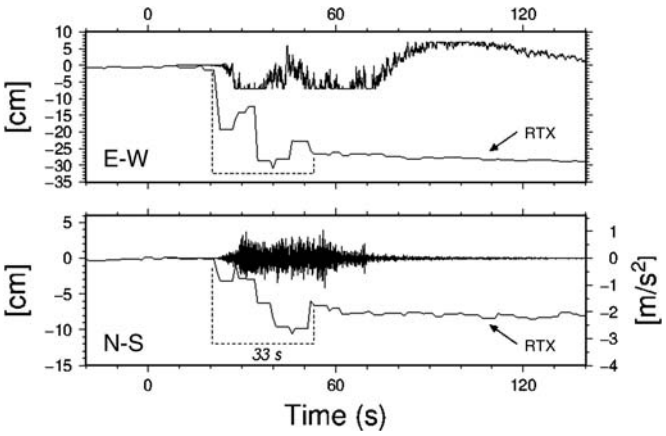

▲ **Figure 4.** First ever real-time detection of coseismic displacement by the RTX capability of a Trimble GNSS device. The easting and northing components, sampled at 1 samples/s, reach −30 and −8 cm, respectively. The east–west (E-W) broadband component is plotted in the top panel. Similarly, the north–south (N-S) acceleration component (about 10%*g* peak ground acceleration) is plotted above the N-S displacement in the lower panel. Assuming that the fault displacement takes place on the subduction interface, for this type of earthquake, due to the geometry of the station source, it is possible to estimate the magnitude—and the slip location—with just one observation site. The permanent static displacement is reached 33 s after the first impulse.

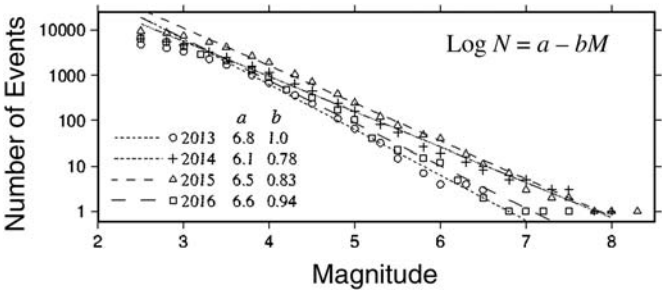

▲ **Figure 5.** Distribution of earthquakes as a function of magnitude for three consecutive years. Aftershock sequences of both Iquique 2014 and Illapel 2015 earthquakes have not been removed.

purposes. A committee of experts was convened by the Ministry of Housing and Urban Development in 2010–2011 to decide on the location of these instruments and installation design. These instruments are Kinemetrics Basalt, with three orthogonal components sampled at 200 samples/s. The range is set to $\pm 4g$ to make sure that even the largest accelerations are recorded on scale. About 70% of these instruments are placed at branches of Carabineros de Chile (Chilean Police) with the majority being connected to their internal communications network. Currently, protocols are being developed to access the remote data from the CSN servers.

Strong-motion records for the two recent **M** > 8 earthquakes, as well as other significant earthquakes taking place in Chile since May 2010, can be downloaded from the website given in Data and Resources. An example of the records of this network, complemented with strong-motion records from the real-time network, can be observed in Figure 6, a product of the 2015 **M** 8.3 Illapel earthquake.

PRELIMINARY RESULTS

To better estimate the fault-slip distribution of large earthquakes, real-time GNSS observations have been incorporated as an integral part of the seismological network. Figure 7 shows the detectability level of earthquakes along the interface between the Nazca and South American plates, considering 4 cm of horizontal displacement at coastal GNSS stations. A scaled source in length, width, and slip is centered at each point on the grid, producing 4 cm of horizontal displacement. It is assumed that these are interplate events.

Along these lines, rapidly available local GNSS data allowed the estimation of the preliminary slip distribution associated with the 16 September 2015 Illapel earthquake (Fig. 8). Only 33 hrs after origin time, a first estimate was published. This is because the stations were not connected in real time, a process that is presently being implemented. Several days later, additional data were included in the inversion scheme and the solution presented a more concentrated patch of slip, roughly maintain the north–south rupture extension.

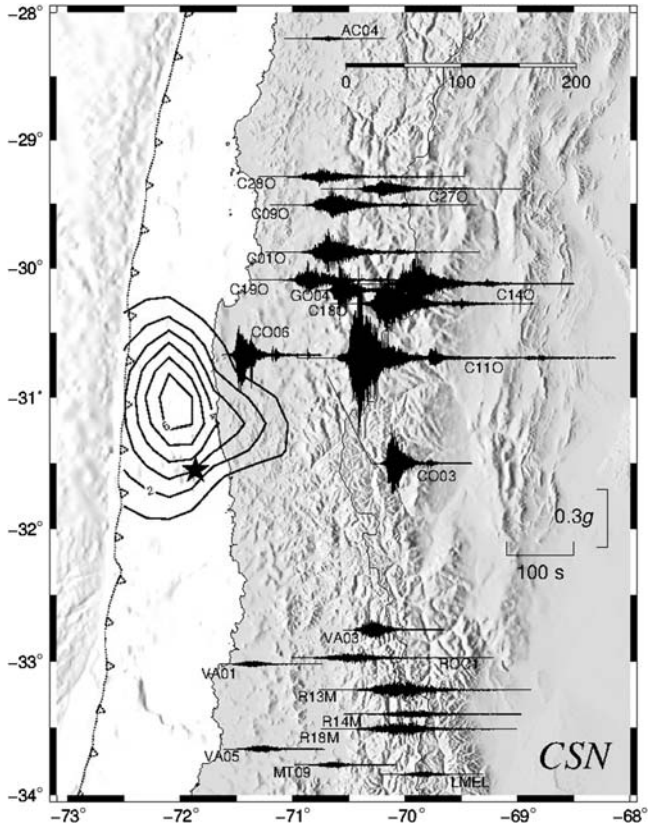

▲ **Figure 6.** Strong-motion records associated with the 15 September M_w 8.4 Illapel earthquake. Maximum accelerations of the order of 60%g were recorded at stations directly inland of the major displacement along the rupture plane.

Additionally, because surface displacements associated with large earthquakes do not saturate in the near field when observed by GNSS devices, Riquelme *et al.* (2016) developed a methodology to rapidly estimate the fault geometry as well as the magnitude of the source in the near field from direct observations of displacement through the W-phase methodology.

SEISMICITY OF CHILE

Denser arrays in northern Chile have been in place for the last 10 yrs (IPOC effort) and 20 yrs in central Chile (metropolitan area) and provide a good basis to delineate main seismic foci within these regions. As an example, Figure 9 shows the corresponding seismicity in central Chile as a result of monitoring of the last few years (CSN catalog, 2017).

Shallow (h < 25 km) seismicity in central Chile during the period 2000–2016 (CSN catalog, 2017) is plotted in Figure 10. Four different concentrations of activity stand out in this figure. The northernmost site (A), with coordinates 32.7° S–71.1° W, corresponds to mine explosions; equivalently, concentration of activity at site B (33.2° S–71.2° W) corresponds to explosions at two copper mines exploiting the same ore; seismic activity at site C is associated with the Tupungatito volcano. The pattern is very similar to that shown by Barrientos

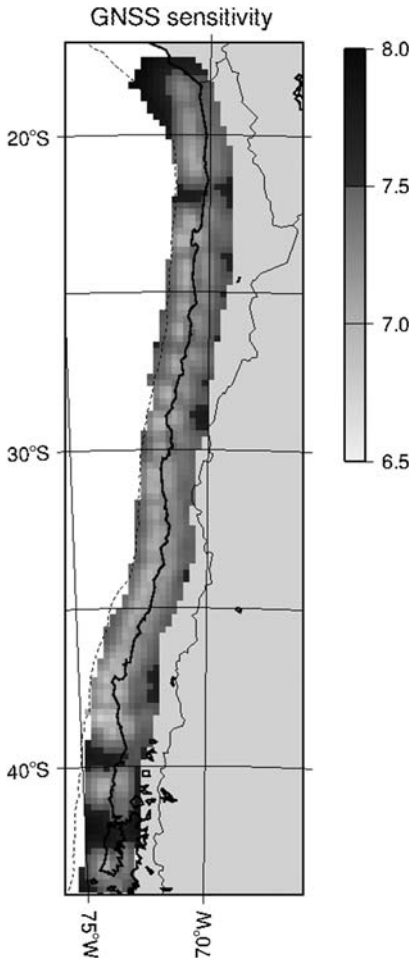

▲ **Figure 7.** Minimum magnitude earthquakes to be detected by a regular GNSS network with a sensitivity of 4 cm, placed at the coast at a 40-km latitudinal spacing, should they occur along the interface contact between the Nazca and South American plates. Darker shades indicate places where events with magnitude over 7.2 should take place to be detected by the network. Minimum magnitude detection for most of the regions offshore is above 6.5.

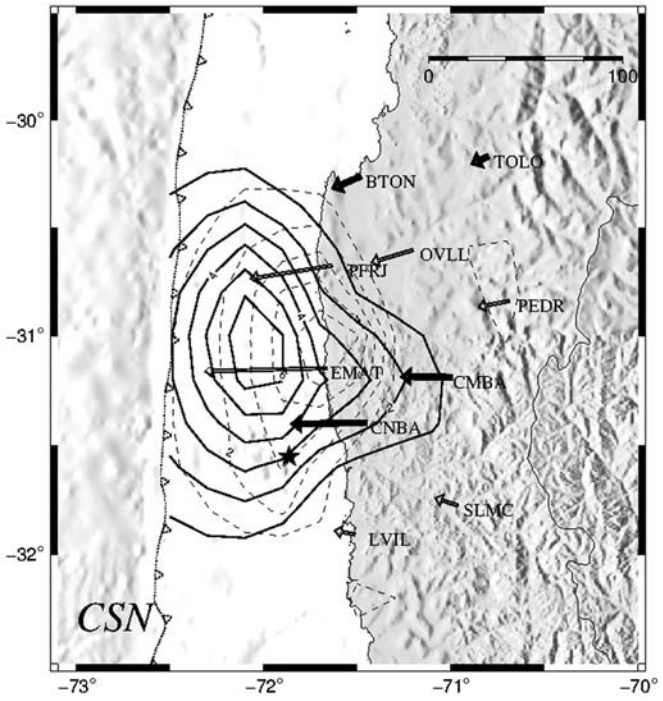

▲ **Figure 8.** Preliminary (dashed lines) and final (solid lines) estimation of slip distribution of the 2015 Illapel earthquake from displacement data observed at the surface (CSN solution) using the Okada (1985) formulation. The first estimation was obtained after 33 hrs of origin time with only four vectors (solid thicker arrows; TOLO, BTON, CMBA, and CNBA). The goal is to diminish this number to few minutes, even including the source duration.

et al. (2004), which included data until 2001, and Pérez *et al.* (2013), with the possible exception of a more defined source region that runs in a north–south orientation along the Olivares River. Seven additional broadband and accelerometers are being installed in the area. This increased monitoring capability is extremely relevant to facilitate the analysis of the potential activity of the San Ramon fault, a geological feature that borders the capital city of Santiago on the western flank of the Andes. This fault has evidenced two stages of activity at about 17,000 and 8000 yrs ago with displacements of few meters each (Vargas *et al.*, 2014).

DISCUSSION

In 2013, the Chilean government tasked the newly created CSN of the University of Chile to operate a real-time network of 65 broadband/strong-motion and 128 Global Positioning System (GPS) stations. In addition, through international partnerships, CSN integrates an additional 35 broadband/strong-motion stations into its operations. When considering existing stations and those part of international agreements of the University of Chile, the BB and accelerograph network comprises over 100 six-component stations distributed throughout the country. Data from all these instruments are transmitted in real time to a central headquarters in Santiago where they are processed, analyzed, distributed, and archived. Data are open and available in real time from the IRIS-Data Management Center (DMC). Currently, the software packages EarlyBird (developed by the West Coast/Alaska Tsunami Warning Center), SeisComP (developed by the GEOFON Program at the Helmholtz Centre Potsdam, GFZ, and Gempa GmbH), and SEISAN (Havskov and Ottemoller, 1999) are used to produce preliminary and final estimations of location and magnitude of earthquakes in Chile within 5 and 20 min of origin time.

To better constrain source parameters of large earthquakes (**M** 7+), the GPS stations are strategically deployed along the coast and near-source zone of large earthquakes. Real-time analysis, archival, and distribution of geodetic data are implemented at the CSN Data Center. In addition to the permanent static deformation analysis approach to rapidly characterize earthquakes, the CSN has adapted the W-phase magnitude estimation methodology to geodetic data (Riquelme *et al.*, 2016), which allows

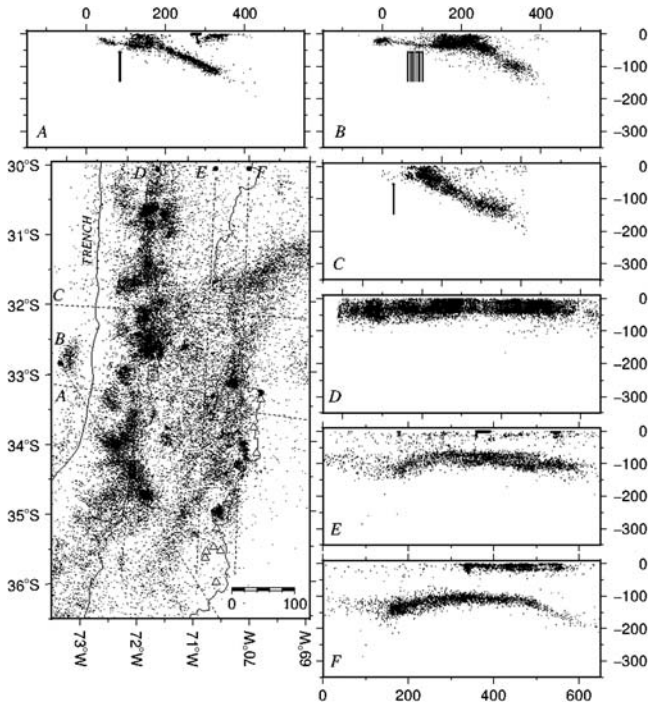

▲ **Figure 9.** Seismicity in central Chile. (Lower left) The map view shows the geographical location of the seismicity for the period 2000–2015. Aftershocks of the 2010 Maule, particularly those associated with the northwest–southeast normal faulting, and Illapel 2015 (close to the coast between 30° and 32° S) events are clear. The six profiles (A–F), spanning a width of 50 km each, along the lines show the subduction interface on an E-W projection (A–C).

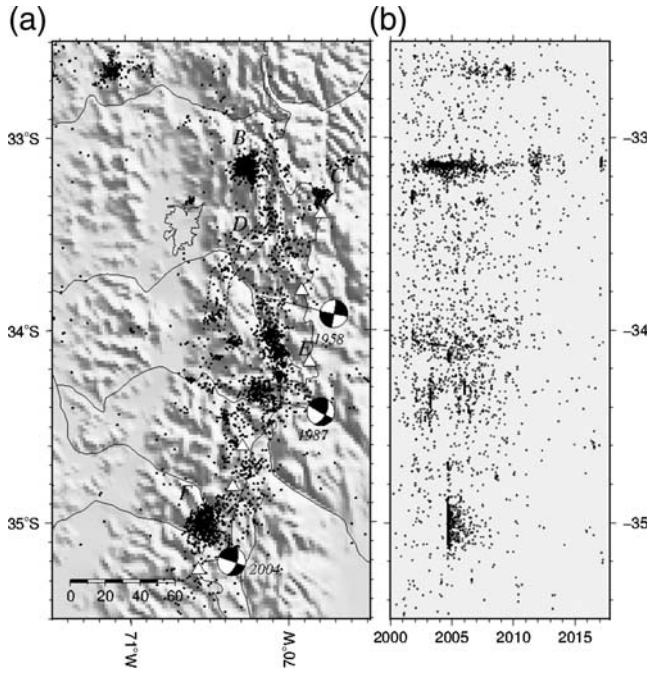

▲ **Figure 10.** (a) Shallow seismicity (hypocentral depths less than 25 km) and (b) its time-dependent behavior in central Chile for the period 2000–2015. Concentration of earthquakes at sites A and B (the northernmost clusters) are the result of mining activity. The seismic activity—located right next to the contour of the city of Santiago at ~33.5° S—is the result of a tunnel construction in that part of town.

the usage of stations even closer to the rupture region than regular broadband techniques. In addition to the real-time system described above, 297 strong-motion offline instruments for engineering purposes complement the network. These instruments have started to produce a significant wealth of accelerograph information generated mainly by the two recent large earthquakes of 2014 (**M** 8.2, Iquique) and 2015 (**M** 8.3, Illapel) earthquakes. Data are publicly available through the CSN webpage (see Data and Resources).

The establishment of this network has unleashed a new era in observational seismology in Chile. The next step is to expand seismological as well as geodetic observations on land as well as the sea floor, above the sources of large tsunamigenic earthquakes. This extension will facilitate further efforts of the CSN on earthquake early warning.

DATA AND RESOURCES

Broadband data in real time are publicly available through the Incorporated Research Institutions for Seismology Data Management Center (IRIS-DMC) under networks C and C1. Strong-motion data for recorded accelerations larger than 2%g are available through the National Seismological Center (CSN) webpage (http://evtdb.csn.uchile.cl, last accessed December 2017). The CSN Catalog of Chilean Seismicity is available upon request or accessed through www.csn.uchile.cl or www.sismologia.cl (last accessed December 2017). All the figures were made using Generic Mapping Tools (www.soest.hawaii.edu/gmt, last accessed December 2017; Wessel and Smith, 1998).

ACKNOWLEDGMENTS

The authors would like to thank Zhigang Peng, Renate Hartog, and an anonymous reviewer for significantly improving this contribution, from content to style.

REFERENCES

Alvarado, P., S. Barrientos, M. Saez, M. Astroza, and S. Beck (2009). Source study and tectonic implications of the historic 1958 Las Melosas crustal earthquake, Chile, compared to earthquake damage, *Phys. Earth Planet. In.* **175,** 26–36.

Barrientos, S. E., and S. N. Ward (1990). The 1960 Chile earthquake: Inversion for slip distribution from surface deformation, *Geophys. J. Int.* **103,** 589–598.

Barrientos, S. E., E. Vera, and T. Monfret (2004). Intraplate seismicity in central Chile, *J. S. Am. Earth Sci.* **16,** 759–768.

Beck, S., S. Barrientos, E. Kausel, and M. Reyes (1998). Source characteristics of historic earthquakes along central Chile subduction zone, *J. S. Am. Earth Sci.* **11,** no. 2, doi: 10.1016/S0895-9811(98)00005-4.

Brenner, J. C. (1911). The seismologic service of Chile, *Bull. Seismol. Soc. Am.* **1,** 25–26.

Cifuentes, I. L. (1989). The 1960 Chilean earthquakes, *J. Geophys. Res.* **94,** 665–680.
Cisternas, M., F. Torrejón, Y. , G. Machuca, M. Lagos, A. Eipert, C. Youlton, I. Salgado, T. Kamataki, M. Shishikura, C. P. Rajendran, *et al.* (2005). Predecessors of the giant 1960 Chile earthquake, *Nature* **437,** 404–407.
Colombelli, S., R. Allen, and A. Zollo (2013). Application of real-time GPS to earthquake early warning in subduction and strike-slip environments, *J. Geophys. Res.* **118,** 3448–3461.
Frohlich, C. (2006). *Deep Earthquakes*, Cambridge University Press, Cambridge, United Kingdom, doi: 10.1017/CBO9781107297562.
Godoy, E., G. Yanez, and E. Vera (1999). Inversion of an Oligocene volcano-tectonic basin and uplifting of its superimposed Miocene magmatic arc in the Chilean Central Andes: First seismic and gravity evidences, *Tectonophysics* **306,** 217–236.
Havskov, J., and L. Ottemoller (1999). SEISAN, earthquake analysis software, *Seismol. Res. Lett.* **70,** 532–534.
Hayes, G., D. Wald, and R. Johnson (2012). Slab1.0: A three-dimensional model of global subduction zone geometries, *J. Geophys. Res.* **117,** no. B01302, doi: 10.1029/2011JB008524.
Kausel, E., and J. Campos (1992). The M_s = 8.0 tensional earthquake of 9 December 1950 of northern Chile and its relation to the seismic potential of the region, *Phys. Earth Planet. In.* **72,** 220–235.
Kinoshita, S., and M. Takagishi (2011). Generation and propagation of static displacement estimated using KiK-net recordings, *Earth Planets Space* **63,** 779–783, doi: 10.5047/eps.2011.05.003.
Klepeis, K. A. (1994). The Magallanes and Deseado fault zones; major segments of South American-Scotia transform plate boundary in southernmost South America, Tierra del Fuego, *J. Geophys. Res.* **99,** 22,001–22,014.
Lemoine, A., R. Madariaga, and J. Campos (2001). Evidence for earthquake interaction in central Chile: The July 1997-September 1998 sequence, *Geophys. Res. Lett.* **28,** 2743–2746.
Lomnitz, C. (1960). A study of the Maipo Valley earthquakes of September 4, 1958, *Proc. of the 2nd World Conf. Earthquake Engineering*, Vol. 1, Tokyo-Kyoto, Japan, 501–520.
Moernaut, J., M. Van Daele, K. Heirman, K. Fontijn, M. Strasser, M. Pino, R. Urrutia, and M. De Batist (2014). Lacustrine turbidites as a tool for quantitative earthquake reconstruction: New evidence for a variable rupture mode in south–central Chile, *J. Geophys. Res.* doi: 10.1002/2013JB010738.
Okada, Y. (1985). Surface deformation due to shear and tensile faults in a half-space, *Bull. Seismol. Soc. Am.* **75,** 1135–1154.
Pardo, M, D. Comte, T. Monfret, R. Boroschek, and M. Astroza (2002). The October 15, 1997 Punitaqui earthquake (M_w = 7.1): A destructive event within the subducting Nazca plate in central Chile, *Tectonophysics* **345,** nos. 1/4, 199–210, ISSN 0040–1951.
Pérez, A., J. A. Ruiz, G. Vargas, R. Rauld, S. Rebolledo, and J. Campos (2013). Improving seismotectonics and seismic hazard assessment along the San Ramon fault at the eastern border of Santiago city, Chile, *Nat. Hazards* doi: 10.1007/s11069-013-0908-3.
Peyrat, S., J. Campos, J. B. de Chabalier, A Perez, S. Bonvalot, M.-P. Bouin, D. Legrand, A. Nercessian, O. Charade, G. Patau, *et al.* (2006). Tarapacá intermediate-depth earthquake (M_w = 7.7, 2005 northern Chile): A slab-pull event with horizontal fault plane constrained from seismologic and geodetic observations, *Geophys. Res. Lett.* **33,** doi: 10.1029/2006GL027710.
Riquelme, S., F. Bravo, D. Melgar, R. Benavente, J. Geng, S. Barrientos, and J. Campos (2016). W phase source inversion using high-rate regional GPS data for large earthquakes, *Geophys. Res. Lett.* **43,** no. 7, 3178–3185.
Smalley, R., I. Dalziel, M. Bevis, E. Kendrick, D. Stamps, E. King, F. Taylor, E. Lauría, A. Zakrajsek, and H. Parra (2007). Scotia arc kinematics from GPS geodesy, *Geophys. Res. Lett.* **34,** L21308, doi: 10.1029/2007GL031699.
Smalley, R., E. Kendrick, M. G. Bevis, I. W. D. Dalziel, F. Taylor, E. Lauría, R. Barriga, G. Casassa, E. Olivero, and E. Piana (2003). Geodetic determination of relative plate motion and crustal deformation across the Scotia–South America plate boundary in eastern Tierra del Fuego, *Geochem. Geophys. Geosys.* **4,** no. 9, 1070.
Thomas, C., R. Livermore, and F. Pollitz (2003). Motion of the Scotia Sea plates, *Geophys. J. Int.* **155,** 789–804.
Tichelaar, B. W., and L. J. Ruff (1991). Seismic coupling along the Chilean subduction zone, *J. Geophys. Res.* **98,** 2017–2038.
Vargas, G., Y. Klinger, T. K. Rockwell, S. L. Forman, S. Rebolledo, S. Baize, R. Lacassin, and R. Armijo (2014). Probing large intraplate earthquakes at the west flank of the Andes, *Geology* doi: 10.1130/G35741.1.
Wang, R., B. Schurr, C. Milkereit, Z. Shao, and M. Jin (2011). An improved automatic scheme for empirical baseline correction of digital strong-motion records, *Bull. Seismol. Soc. Am.* **101,** no. 5, 2029–2044.
Wessel, P., and W. H. F. Smith (1998). New, improved version of Generic Mapping Tools released, *Eos Trans. AGU* **79,** 579.

S. Barrientos
National Seismological Center (CSN) Team
Facultad de Ciencias Físicas y Matemáticas
Universidad de Chile
Beauchef 850
Santiago, Chile
sbarrien@csn.uchile.cl

Published Online 14 February 2018